



HAL
open science

Simulation of an Early Warning Fire System

Paulo Lourenço, Alessandro Fantoni, Manuela Vieira

► **To cite this version:**

Paulo Lourenço, Alessandro Fantoni, Manuela Vieira. Simulation of an Early Warning Fire System. 10th Doctoral Conference on Computing, Electrical and Industrial Systems (DoCEIS), May 2019, Costa de Caparica, Portugal. pp.305-317, 10.1007/978-3-030-17771-3_27. hal-02295235

HAL Id: hal-02295235

<https://inria.hal.science/hal-02295235>

Submitted on 24 Sep 2019

HAL is a multi-disciplinary open access archive for the deposit and dissemination of scientific research documents, whether they are published or not. The documents may come from teaching and research institutions in France or abroad, or from public or private research centers.

L'archive ouverte pluridisciplinaire **HAL**, est destinée au dépôt et à la diffusion de documents scientifiques de niveau recherche, publiés ou non, émanant des établissements d'enseignement et de recherche français ou étrangers, des laboratoires publics ou privés.



Distributed under a Creative Commons Attribution 4.0 International License

Simulation of an Early Warning Fire System

Paulo Lourenço^{b,c}, Alessandro Fantoni^{a,c}, Manuela Vieira^{a,c}

^aISEL - Instituto Superior de Engenharia de Lisboa, Instituto Politécnico de Lisboa
Rua Conselheiro Emídio Navarro, 1, 1959-007 Lisboa, Portugal;

^bFaculdade de Ciências e Tecnologia, FCT, Universidade Nova de Lisboa
Departamento de Engenharia Eletrotécnica, Campus da Caparica, 2829-516 Caparica, Portugal;

^cCTS-UNINOVA, Departamento de Engenharia Eletrotécnica, Faculdade de Ciências e Tecnologia, FCT,
Universidade Nova de Lisboa, Campus da Caparica, 2829-516 Caparica, Portugal
pj.lourenco@campus.fct.unl.pt

Abstract. In this paper, we will be using separate software tools (wireless network and Finite Differences Time Domain based simulators) to simulate the implementation of a wireless sensor network model based on low-rate/power transmission technology. The system operates in an unlicensed frequency range and the sensing nodes rely on surface plasmon resonance phenomenon for the detection of combustion by-products. More specifically, our simulations contemplate a system for early detection of fire in densely forested areas, which will then issue a warning in an automated way. As late detection of these events usually leads to severe flora, terrain, wild life and societal impact, an early warning system will provide better event assessment conditions, thus enabling efficient resources allocation, adequate response and would certainly be a promising improvement in minimizing such disruptive impairments.

Keywords: FDTD simulations, MMI coupler, surface plasmon resonance, WSN, fire detection

1 Introduction

Contemporaneous technologies on wireless mobile communication, embedded systems, cloud computing and sensors, have contributed for many examples of successful applications where intelligent systems have been employed. Implementations of such systems have occurred in many sectors of our economy, from public security systems to logistics platforms and many other, and it is predictable a worldwide proliferation of these devices/systems in many aspects of our daily lives, providing ubiquitous and seamless access to a smart world. This transition will require the development of an enormous quantity of such devices, all with energy and manufacturing requirements, hence all efforts must be made to assure cost-effective and highly efficient approaches at both their production and usage/operation cycles [1].

The paradigm associated to a smart world, the internet of everything (IoE), makes reference to a *network* of interconnected *things*. Here, the *network* is usually contemplated as the TCP/IP network we all rely on at present time and the *things* being a myriad of sensors and actuators. All of these devices incorporate telecommunications, storage and processing capabilities, as depicted in **Fig. 1**, thus being able to provide human to machine and/or machine to machine interactions. They are also able to aggregate themselves as a network of smart nodes which is then bridged with traditional communications networks or the Internet through a gateway, enabling this way remote operation, control and management [2].

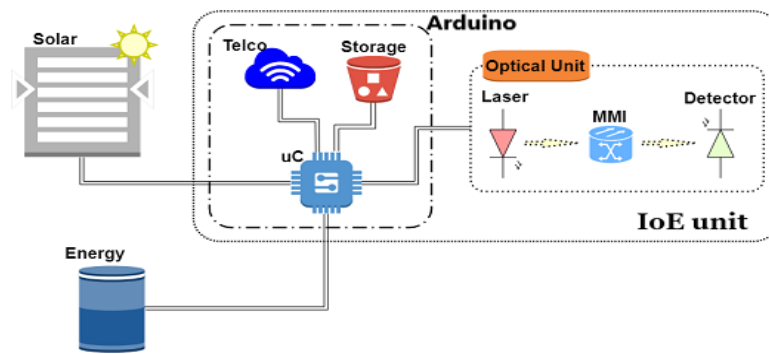


Fig. 1. Proposed block diagram of a single unit.

This document intends to initiate the steps for the development of a highly integrated, efficient and cost effective Information and Communication Technology (ICT) system for early detection of wild fire in forested areas. Towards that end and through available software tools [3], [4], the simulation of the three components of this work have been conducted. Namely:

- The SPR based sensor which is able to sense minute variations of its surrounding environment refractive index. As such, the resulting by-products of burning wood (e. g. soot – carbon atoms agglomerates) will be detected as an increase in the refractive index of the environment in the near proximity of the sensing structure;
- The 3 dB optical coupler that will provide the required optical paths for the detection and reference fields of our device. These EM fields will be analysed, processed and quantified, and the obtained results will be monitored and interpreted;
- The Wireless Sensor Network (WSN) that enables the deployment of these devices over an arbitrary area, allowing control, monitoring and interconnection between

all the network nodes, hence providing an early warning system for wild fire in forests, in an automated way.

The remaining of this paper is organized as follows:

- Next section presents how this document relates to the context of Innovation in Industry and Service Systems, which is the main focus of DoCEIS2019 Doctoral Conference;
- Then follows the Surface Plasmon Resonance section, where numerical simulations of the sensing structure of each individual device are presented and the results obtained show the ability to detect refractive index variations of the surrounding environment. The refractive index increase will result from the burning wood smoke carrying, amongst other compounds, unignited and condensed micro-meter sized agglomerates of carbon atoms (soot), which move away from fire and will increase the refractive index of the environment near the sensing structures. This soot production results from unburned carbon atoms that moving away from the top of the flame and is still an active field of research [5].
- Follows Multimode Interference (MMI) section, where will be described a 1×2 MMI structure consisting on a 3 dB coupler that provides the required optical paths to feed the sensing device and to yield the reference arm signal for further analysis and processing.
- Afterwards comes the Wireless Sensor Network (WSN) section. In this section will be presented a software tool [6] that assisted on the deployment of the nodes on the map location, the network structure organization, the communication between nodes, the communication with the external network (i. e. TCP/IP) and the whole network behaviour simulation in a fire event.
- Finally, there is the Conclusions section where obtained results are gathered, analysed and conclusions are drawn and reported. Here, future areas of related research will also be discussed. Namely, the experimental implementation of simulated device and the optimization and development of software functions in the WSN simulator tool.

2 Contribution to Innovation in Industry and Service Systems

ICT systems have been playing an important and increasing role for several years, as far as reliable control of automated tasks is concerned and in many sectors of contemporaneous society. Even in traditional sectors of our economy, technological proliferation is a fact and the trend seems to indicate an increasing penetration in every aspect of our lives. Industry will be no exception to this tendency and is forecasted to undergo a major transformation already on its way. This is expected to be a profound industrial revolution that will take manufacturing processes automation to a whole new level of efficiency and mass production. Although the debate about how to designate this

transformation is still in progress, the term “Industry 4.0” has been agreed upon amongst many western European companies, academics and technological practitioners.

According to [7], the most often cited terms when referring to Industry 4.0 are Cyber-Physical Systems (CPS), Internet of Things (IoT), Smart Factory (SF), and Internet of Services (IoS). CPS aims the integration of physical systems with computation, IoT is mainly about technological systems being able to exchange data while sensing their surroundings, IoS intends to wrap existing and future connected mobile devices as gateways to services provided by the manufacturer and SF aggregates CPS and IoT to seamlessly assist machines and humans to perform their manufacturing tasks.

In this article we would like to point out Innovation also as a key element in Industry 4.0 for all these interacting systems certainly provide a fertile platform in which originality will thrive. To this end, our simulations envisions an automated early warning fire detection system consisting on a WSN with integrated optical devices based on SPR for the detection of burning wood by-products, namely soot. To the best of our knowledge, this fire detection system represents a novel approach to wildfire events prevention in forests and their severe environmental, financial and societal impact.

The automated early warning fire detection system is a clear implementation of real world virtual integration where live data is gathered, exchanged, analysed and decisions are made based on this process, thus entailing the set of recommendations for Industry 4.0 referred in the literature. Moreover, the same working principle of this system might be applied in similar devices but to sense other physical quantities, as long as they can be translated into refractive index variations of the environment in the vicinity of the sensing structure.

3 Surface Plasmon Resonance

Optical sensing devices based on the excitation of plasmonic waves on metallic surfaces are usually referred as Surface Plasmon Resonance (SPR) sensors and their operation relies on the detection of refractive index variations in the electromagnetic (EM) mode supported by the free electrons of the metallic surface. These structures have been extensively reported as valid applications for the detection of gases, chemical and biological elements.

The scientist who first described this phenomenon used a structure that has been named after him, the Kretschmann configuration [8]. This method consists on a quartz prism where an incident EM field is refracted on a facet and reflected at the base where a thin metallic film has been deposited. Under the right conditions, the energy of the incident field is transferred to the free electrons on the metallic surface and triggers their oscillation. These oscillations generate surface plasmon waves that propagate along the metal/dielectric interface.

Surface plasmon waves are highly sensitive to the refractive index of the surrounding environment. This wave is a single transverse magnetic (TM) mode and its magnetic field intensity vector is parallel to the metal/dielectric interface plane and perpendicular to the propagation direction. Its propagation constant can be defined as:

$$\beta_{SP} = k_0 \sqrt{\frac{\epsilon_m \epsilon_d}{\epsilon_m + \epsilon_d}}. \quad (1)$$

where β_{SP} is the propagation constant of the surface plasmon wave, k_0 is the vacuum wavenumber and ϵ_m and ϵ_d are the dielectric permittivity for metal and insulator, respectively. As one can infer through the above equation, this propagation constant is highly sensitive to minor variations on the refractive index of the surrounding environment [9].

Our numerical simulations consisted on a Silicon Carbide (SiC) waveguide deposited over a layer of silica (SiO₂) and where a 50 nm high layer of Aluminium (Al) is deposited. The structure was dimensioned to assure single mode operation at 633 nm wavelength at initial waveguide dimensions, then its cross section is increased to create a bimodal waveguide as shown in **Fig. 2**. The working principle is, to some extent, similar to the device developed by Zinoviev et al. [10] for the interferometric biosensor.

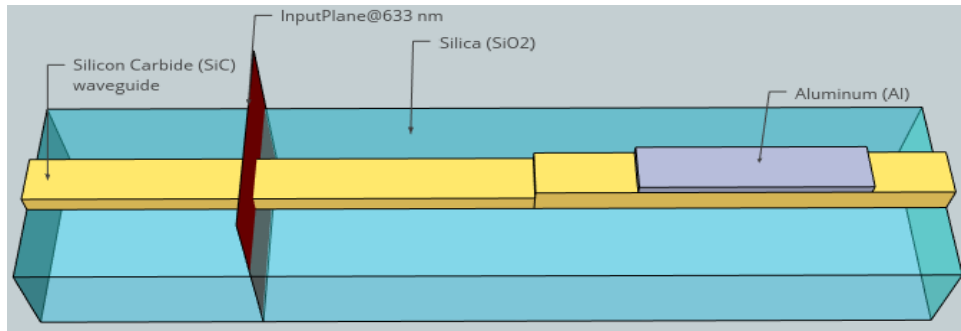


Fig. 2. Diagram of the simulated structure.

The reasons justifying the selection of SiC as the material for the waveguide and Al for metallic layer were its almost non-existent absorption at visible wavelengths for the former and its cost effectiveness for the latter. Moreover, the minute dimensions of the structure enable the integration of all components in one single device, thus fully complying with the lab-on-chip concept [11].

Numerical simulations of this structure based on the Finite Differences Time Domain algorithm were carried out. This 3D structure is an invariant refractive index structure on the third axis and the waveguide is much wider than thick. Thus, one may assume the modal fields having the same behaviour along its width, hence a 2D planar waveguide approach might be considered [12]. Nevertheless, given the high contrast involved and

being a rectangular waveguide, the dual effective-index method [13] was the considered approach and the results obtained were successfully compared with the ones provided by analysis for this structure [14].

The equivalent 2D simulation workspace is depicted in **Fig. 3**, where in **a)** is depicted a longitudinal cut of simulated structure and in **b)** one can identify the refractive index of the core waveguide, the two propagation modes (i. e. TM_0 and TM_1) allowed in the wider cross section of this structure, the modes profile and their amplitudes.

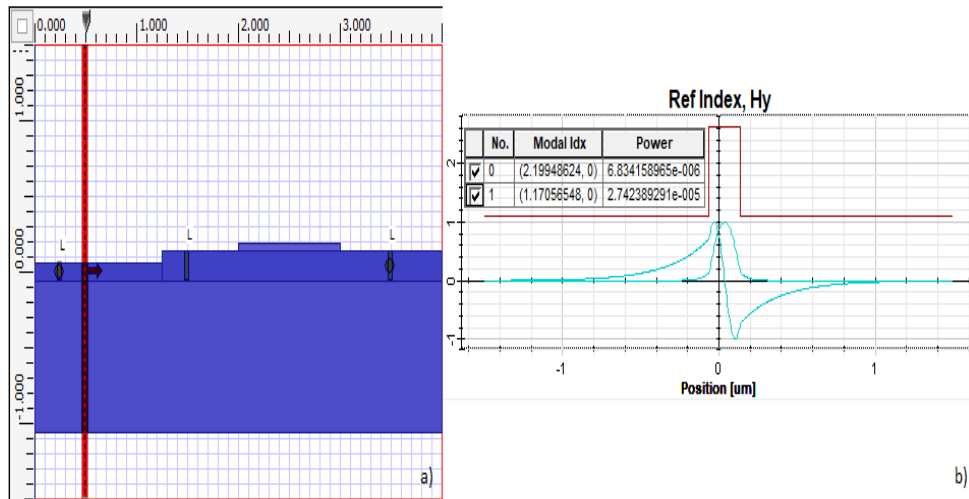


Fig. 3.a) OptiFDTD simulation workspace; **b)** Refractive index profile, modes propagated and respective power amplitudes.

Note that the mode amplitude of TM_0 is approximately half the amplitude of TM_1 , therefore contribution of the fundamental mode for transmission is minimal. Moreover, simulations show that TM_0 is highly dispersed into the SiO_2 substrate and only reminiscent power reaches the detection area. With this in mind, following procedure and discussion considered only the propagation of TM_1 mode.

The Al layer has been simulated considering the Lorentz-Drude dispersive model from OptiFDTD [3] library, thus providing the closest possible conditions to experimental environment. **Fig. 4.a)** shows a close up of the Poynting vector evolution along the propagation direction. It is noticeable the propagation of the SPR wave along the Al layer. After the sensing area, the field amplitude decays approximately 6 dB, as can be verified in **b)** where are shown the obtained field profiles on the observation lines located before and after this zone.

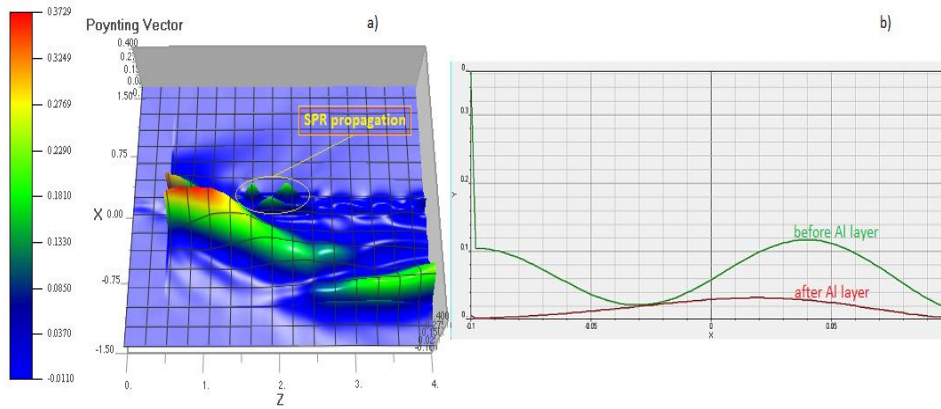


Fig. 4.a) Poynting vector amplitude evolution; b) Field profiles before and after detecting zone.

This sensing structure must be able to detect slight refractive index variations in its close vicinity. To evaluate its detection capabilities, a similar conditions simulation took place only this time with an increase of 0.1 in the refractive index of the surrounding environment. The results obtained are presented in Fig. 5, where are shown the transmission spectral response for both default and increased refractive indexes and has been verified a red shift of $\sim 7.4 \text{ nm}$ for a variation of 0.1 refractive index units.

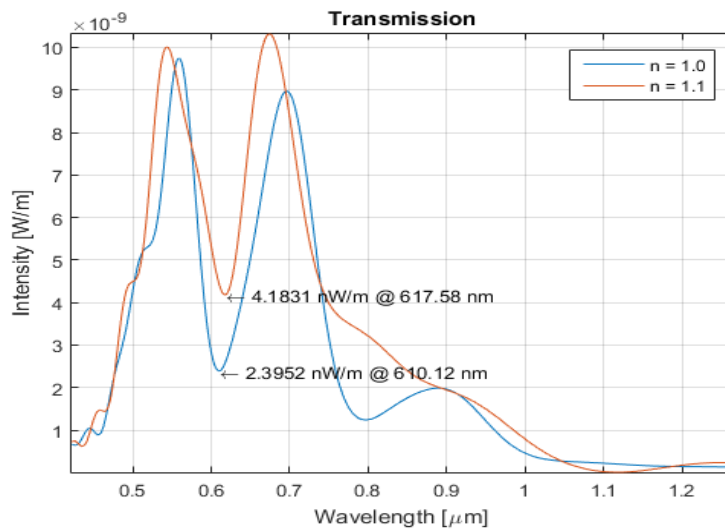


Fig. 5. Transmission spectral response for both refractive indexes.

Burning wood produces large quantities of smoke carrying droplets of soot that is formed by unburned and condensed micro-meter sized agglomerates of carbon atoms [5]. Carbon refractive index is 2.4105 at the operating wavelength of 633 nm [15] thus, production of these carbon agglomerates (soot) that result from the combustion of wood will contribute for the refractive index increase in the surrounding environment of the detection unit.

4 Multimode Interference

Our intent was to obtain two identical EM field profiles resulting from an initial fundamental mode input profile. One of the EM fields will be affected by a sensing area and the other one will represent a comparison reference for further processing.

The available options evaluated were single mode Y-junctions, two-mode interference (TMI) and MMI devices, but they all presented disadvantages when compared to the latter structure. Namely, close proximity of access waveguides on these devices usually leads to unwanted modal coupling and separation aperture filling, due to the limited resolution of lithographic process, hence affecting TMI section length arbitrarily and causing performance degradation [16]. According to [17]–[19], operation of MMI devices relies on the self-imaging principle which states that single or multiple images of a given input field profile are replicated periodically in space, as the electromagnetic field propagates through the waveguide. The propagation constant of a mode β_m ($m = 0, 1, 2, \dots$) propagating in a high contrast step index multimode device shows an approximate quadratic dependence to the mode number m :

$$\beta_m \cong k_0 n_{core} - \frac{(m+1)^2 \pi \lambda_0}{4 n_{core} W_{eff}^2}, \quad (2)$$

where k_0 is the vacuum wavenumber, n_{core} the refractive index of the structure, λ_0 the vacuum wavelength and W_{eff} the effective width of the MMI waveguide (considering the Goos-Hänhchen shift on the device boundaries). In high refractive index contrast devices, the penetration depth of the EM field beyond the inner walls of the device is practically non-existent, hence:

$$W_{eff} \cong W \quad (3)$$

The spatial location of single/multiple and direct/mirrored images, resulting from the propagation modes interference, is directly related to the beat length of the two lowest order modes, L_π :

$$L_\pi = \frac{\pi}{\beta_0 - \beta_1} \cong \frac{4 n_{core} W_{eff}^2}{3 \lambda_0} \quad (4)$$

Single mirrored and direct images from the input field profile form at $3L_\pi$ and $2(3L_\pi)$, respectively, while two-fold images form at $\frac{1}{2}(3L_\pi)$ and $\frac{3}{2}(3L_\pi)$. The single images are approximately the same amplitude as the input EM field and each of the two-fold images is affected by an attenuation factor of 3 dB , thus offering the ideal conditions for a 3 dB coupler device, similar to the structure diagram depicted in Fig. 6.

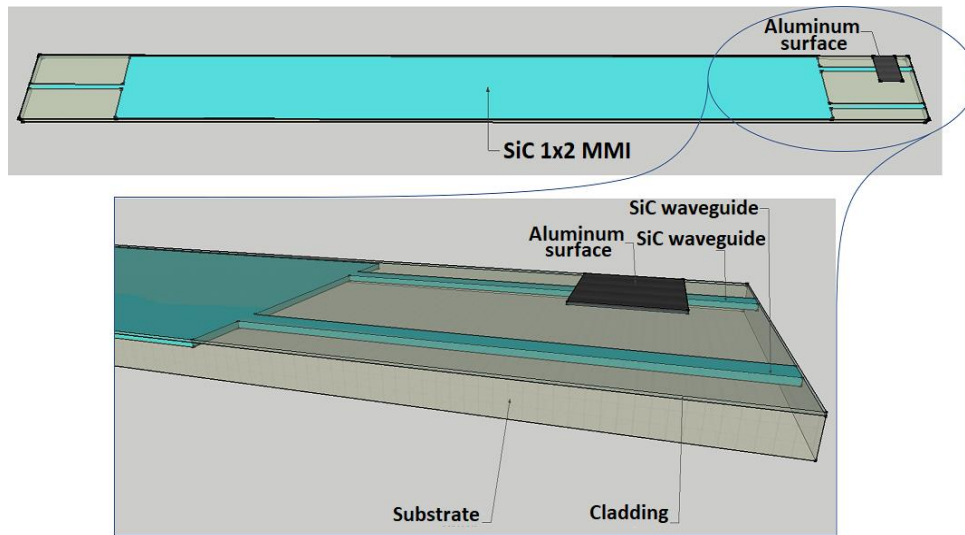


Fig. 6. MMI structure and sensing area diagram.

The simulated device consisted on a silicon carbide (SiC) based structure, where the input and output waveguides were dimensioned to support single mode operation at 633 nm vacuum wavelength. First simulations of our structure did not show the intended results, mainly due to fine misplacement of the output waveguides, thus an optimization algorithm had to be executed on the simulation tool.

The results obtained are shown in Fig. 7, where one is able to find the optical field profile spatial distribution on the top half of the figure and, at the bottom half, the normalised amplitudes along the monitored paths leading to the output waveguides. Note that, at the latter, there are two evolving lines that reflect each of the already mentioned paths. These are hardly distinguishable due to the optimization algorithm that balanced the amplitudes of both output waveguides.

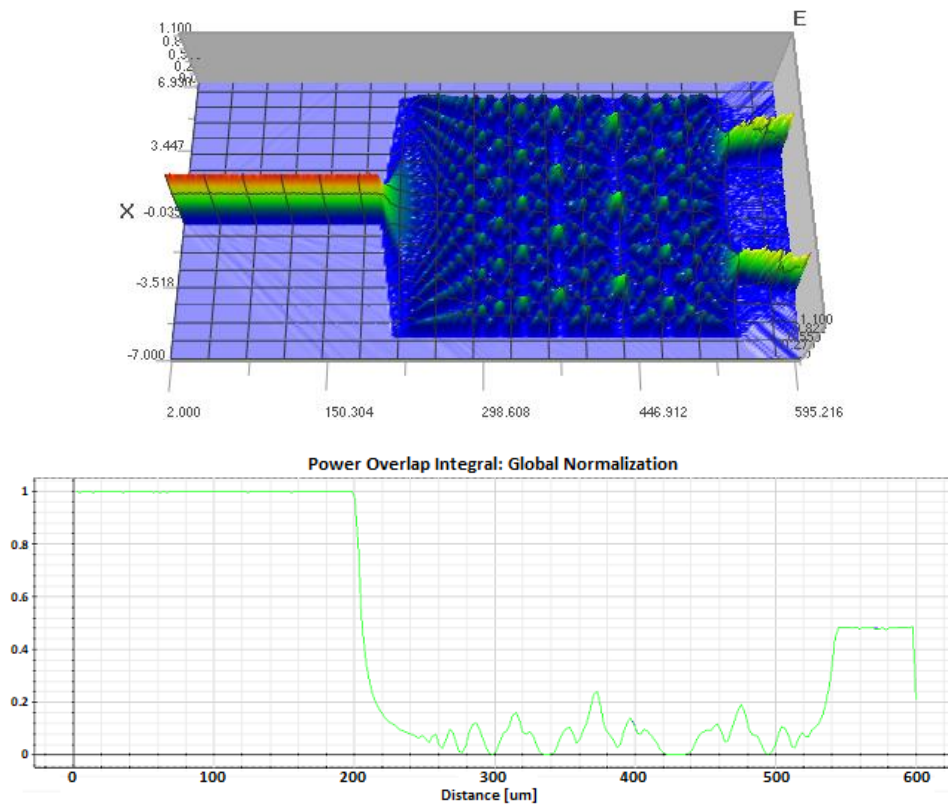


Fig. 7. Optical field profile distribution (top) and field amplitudes along the monitoring paths (bottom).

5 Wireless Sensor Network

Contemporaneous state-of-the-art technology in telecommunications and electronics enables the development of a myriad of sensor structures, each with capabilities of sensing specific events in its proximity, communicating with its neighbours, data storage and processing power. With this in mind, a large number of these devices deployed over an arbitrary area can collaborate to form an *ad-hoc* network of sensing nodes, which will be referred throughout this document as a Wireless Sensor Network (WSN).

The trend direction seems to point for these WSNs to be present in every aspect of our lives as the predominant sensing technology [2], with unprecedented impact in every sector of our economy and in society. Implementation and deployment of a WSN is not

burden free and its cost is directly related to the number of nodes in the network. Hence, it is of vital importance to define an implementation strategy prior to deployment. To this end, network simulators are of great assistance for they enable the simulation and refinement of the network architecture, operation and behaviour of our design before going into the implementation phase.

To elaborate this document, several network simulators were evaluated, namely Packet Tracer [20], NS-2 [21] and CupCarbon [4]. After consulting the available documentation for each tool and careful consideration, the selected simulator was the latter one for its appropriateness over our intended task: - WSN simulation for early fire detection. CupCarbon [22] is a simulator that operates at the application layer of the nodes and will be next demonstrated adequate for network behavioural monitoring when in presence of a fire event. It integrates radio propagation and interference models which allows fast and accurate evaluation of link quality based on transmission conditions [23]. Sensor nodes can be placed on an actual geographical map through Open Street Map (OSM) framework.

Being a multi-agent and discrete event simulator it enables monitoring several node related events, such as tracking mobility, energy consumption, gas and fire detection, and more, while simulation is running [24]. Moreover, this software is able to simulate IEEE 802.15.4 (Zigbee) [22], WiFi and LoRA, and each node has data processing capabilities through SenScript commands. It is an open source Java programmed tool, source code is available and may be altered to include custom code, functions or algorithms, e. g. an improved Dijkstra algorithm [25] or data mining techniques for fire detection [26].

Thus, CupCarbon was the selected simulator to model an automated early detection of fire in forests based on a WSN. The selected radio protocol was Zigbee for this is a low-rate, low-traffic network and distance between nodes is not limited by radio but sensing range. To this end, 178 nodes with 50 m sensing range were deployed over a densely forested area, all with data storage and processing capabilities. Nodes distribution was maximized on tree areas over bushes or clear sight terrain. **Fig. 8** shows the deployed WSN where each orange dot is a sensing node, the orange triangle is the sink and the white arrows symbolize bi-directional links.



Fig. 8. Deployed WSN.

A gateway (sink) was placed within reach of some nodes to assure interaction with the external network (TCP/IP), thus allowing remote control, monitoring and management of all network elements. Scripts were developed for both nodes and gateway, according to their operational functions:

- Nodes are always checking the radio data buffer for an incoming message to route and, at every given time set in the script, the sensing device is monitored for an alarm condition. They only transmit or forward a message once and wait for the reset message from the gateway;
- Gateway receives messages from nodes and forwards them to the external network. This is signalled by a yellow circle around the triangle. Once an alarm message is received from all neighbours, the sink sends the reset message to nodes. Sink also provides application layer connection for remote control, monitoring and management of all WSN.

Simulation was conducted and, at some point in time, a fire event has been modelled. Figure 9 depicts the start of the fire event detected by the sensing structure. Then, the alarm message is sent out the node to its neighbours and starts propagating to the rest of the network. As the message evolves throughout the network, after 61 received messages it reaches the gateway, as represented in Figure 10, and is forwarded through an available technology (e. g. 3G/4G, cable, optical fibre, ADSL, etcetera) to the remote control centre for evaluation.

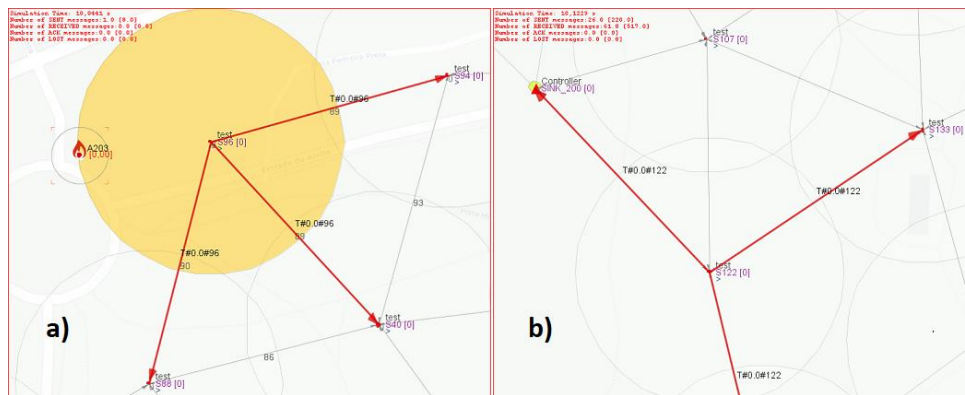


Fig. 9.a) Fire event start and initial alarm message propagation; **b)** Alarm message propagation reaches gateway.

6 Conclusions

The simulated SPR based sensing device, has been designed on a SOI platform with cost-effective materials such as Al for the active metal and SiC for the waveguide and MMI

elements. This structure was able to detect refractive index variations of the surrounding environment at visible wavelengths, thus its features can be incorporated on an experimental sensing device. This structure has been modelled with dispersive materials, including losses, to reflect as much as possible experimental conditions. Device integration of one or many of these structures is achievable given design simplicity and involved minute dimensions, thus complying with lab-on-chip concept [7]. Simulations of a network operating under these conditions have shown that an early wild fire detection system is feasible when implemented on a WSN.

Future work will consist on the experimental implementation (through Plasma Enhanced Chemical Vapour Deposition facilities at ISEL) of the sensing device to validate the results obtained, setting up a comparison benchmark between mentioned results and the ones obtained with noble metals and will also consider development of Java based code in the WSN simulation tool, in order to optimize energy monitoring capabilities in a more consistent way and to develop a fire spreading algorithm.

Acknowledgments. This research was supported by EU funds through the FEDER European Regional Development Fund and by Portuguese national funds by FCT – Fundação para a Ciência e a Tecnologia with projects PTDC/NAN-OPT/31311/2017, SFRH/BPD/102217/2014 and by IPL IDI&CA/2018/aSiPhoto. A special word of recognition to professors Miguel Fernandes and Yuri Vygranenko, whom have contributed with their invaluable expertise.

References

- [1] H. N. Saha, A. Mandal, and A. Sinha, “Recent trends in the Internet of Things,” *2017 IEEE 7th Annu. Comput. Commun. Work. Conf. CCWC 2017*, pp. 15–18, 2017.
- [2] S. Kaur and V. Grewal, “Wireless Sensor Networks- Recent Trends and Research Issues,” *Indian J. Sci. Technol.*, vol. 9, no. 48, pp. 1–5, 2017.
- [3] “Design software for photonics.” [Online]. Available: <https://optiwave.com>. [Accessed: 29-Dec-2018].
- [4] “CupCarbon, WSN simulator.” [Online]. Available: <http://www.cupcarbon.com/>. [Accessed: 29-Dec-2018].
- [5] H. W. Emmons and A. Atreya, “The science of wood combustion Howard W Emmons and Arvind Atreya heat ’ heat transfer fuel mass transfer,” vol. 5, no. December, pp. 259–268, 1982.
- [6] Virtualys, IEMN, IRCICA, Xlim, and Lab-STICC, “CupCarbon User Guide,” 2017.
- [7] M. Hermann, T. Pentek, and B. Otto, “Design Principles for Industrie 4.0 Scenarios: A Literature Review,” *Technische Universität Dortmund*, no. 01, 2018.
- [8] E. Kretschmann and H. Raether, “Radiative Decay of Non Radiative Surface Plasmons Excited by Light,” no. November 1968, pp. 0–1, 1968.
- [9] J. Homola, “Surface Plasmon Resonance Sensors for Detection of Chemical and Biological Species,” *Chem. Rev.*, vol. 108, pp. 462–493, 2008.

- [10] K. E. Zinoviev, A. B. González-Guerrero, C. Domínguez, and L. M. Lechuga, "Integrated bimodal waveguide interferometric biosensor for label-free analysis," *J. Light. Technol.*, vol. 29, no. 13, pp. 1926–1930, 2011.
- [11] S. Haeberle, D. Mark, F. Von Stetten, and R. Zengerle, "Microfluidic platforms for lab-on-a-chip applications," *Microsystems Nanotechnol.*, vol. 9783642182, no. 9, pp. 853–895, 2012.
- [12] J. Buus, "The Effective Index Method and Its Application to Semiconductor Lasers," *IEEE J. Quantum Electron.*, vol. 18, no. 7, pp. 1083–1089, 1982.
- [13] K. S. Chiang, "Dual effective-index method for the analysis of rectangular dielectric waveguides," *Appl. Opt.*, vol. 25, no. 13, p. 2169, 1986.
- [14] "Computational Photonics." [Online]. Available: <https://www.computational-photonics.eu/eims.html>. [Accessed: 29-Dec-2018].
- [15] "Refractiveindex.info database," 2017. [Online]. Available: <http://refractiveindex.info/>. [Accessed: 29-Dec-2018].
- [16] L. B. Soldano, F. B. Veerman, M. K. Smit, B. H. Verbeek, A. H. Dubost, and E. C. M. Pennings, "Planar Monomode Optical Couplers Based on Multimode Interference Effects," *J. Light. Technol.*, vol. 10, no. 12, pp. 1843–1850, 1992.
- [17] L. B. Soldano and E. C. M. Pennings, "Optical Multi-Mode Interference Devices Based on Self-Imaging : Principles and Applications," *J. Light. Technol.*, vol. 13, no. 4, 1995.
- [18] Honbun, "Chapter 2 Multimode Interference Theory," 2006, pp. 15–64.
- [19] A. Sosa, "Design of Silicon photonic Multimode Interference Couplers," *Opt. Express*, vol. 19, no. 2, p. 88, 2012.
- [20] "Cisco Packet Tracer." [Online]. Available: https://www.netacad.com/courses/packet-tracer/download/?p_auth=h6jOI2lZ&p_p_auth=iJXrHgDA&p_p_id=resendscreename_WAR. [Accessed: 29-Dec-2018].
- [21] "NS-2." [Online]. Available: <https://www.isi.edu/nsnam/ns/>. [Accessed: 29-Dec-2018].
- [22] A. Bounceur, "CupCarbon: A New Platform for Designing and Simulating Smart-City and IoT Wireless Sensor Networks (SCI-WSN)," *Proc. Int. Conf. Internet Things Cloud Comput.*, no. March, p. 1:1--1:1, 2016.
- [23] A. Bounceur *et al.*, "CupCarbon: A new platform for the design, simulation and 2D/3D visualization of radio propagation and interferences in IoT networks," *CCNC 2018 - 2018 15th IEEE Annu. Consum. Commun. Netw. Conf.*, vol. 2018–Janua, no. April, pp. 1–4, 2018.
- [24] K. Mehdi, M. Lounis, A. Bounceur, and T. Kechadi, "CupCarbon: A Multi-Agent and Discrete Event Wireless Sensor Network Design and Simulation Tool," in *Proceedings of the Seventh International Conference on Simulation Tools and Techniques*, 2014.
- [25] C. Lopez-Pavon, S. Sendra, and J. F. Valenzuela-Valdes, "Evaluation of CupCarbon Network Simulator for Wireless Sensor Networks," *Netw. Protoc. Algorithms*, vol. 10, no. 2, p. 1, 2018.
- [26] M. Saoudi, A. Bounceur, R. Euler, and T. Kechadi, "Data Mining Techniques Applied to Wireless Sensor Networks for Early Forest Fire Detection," in *Proceedings of the International Conference on Internet of things and Cloud Computing - ICC '16*, 2016, no. Dm, pp. 1–7.